



Sensorless Fault Tolerant Control for Induction Motors

Nadia Djeghali, Malek Ghanes, Said Djennoune, Jean-Pierre Barbot

► To cite this version:

Nadia Djeghali, Malek Ghanes, Said Djennoune, Jean-Pierre Barbot. Sensorless Fault Tolerant Control for Induction Motors. International Journal of Control, Automation and Systems, 2013, 11 (3), pp.563-576. 10.1007/s12555-012-9224-z . hal-00923749

HAL Id: hal-00923749

<https://inria.hal.science/hal-00923749>

Submitted on 4 Jan 2014

HAL is a multi-disciplinary open access archive for the deposit and dissemination of scientific research documents, whether they are published or not. The documents may come from teaching and research institutions in France or abroad, or from public or private research centers.

L'archive ouverte pluridisciplinaire **HAL**, est destinée au dépôt et à la diffusion de documents scientifiques de niveau recherche, publiés ou non, émanant des établissements d'enseignement et de recherche français ou étrangers, des laboratoires publics ou privés.

Sensorless Fault Tolerant Control for Induction Motors

Nadia Djeghali, Malek Ghanes, Said Djennoune, and Jean Pierre Barbot

Abstract: In this paper, a sensorless fault tolerant controller for induction motors is developed. In the proposed approach, a robust controller based on backstepping strategy is designed in order to compensate both the load torque disturbance and the rotor resistance variations caused by the broken rotor bars faults. The proposed approach needs neither fault detection and isolation schemes nor controller reconfiguration. Moreover, to avoid the use of speed and flux sensors, a second order sliding mode observer is used to estimate the flux and the speed. The used observer converges in finite time and permits to give good estimates of flux and speed even in presence of rotor resistance variations and load torque disturbance. Since the used observer converges in finite time, the stability of the closed-loop system (controller + observer) is shown in two steps. First, the boundedness of the closed-loop system trajectories before the convergence of the observer is proved. Second, the convergence of the closed-loop system trajectories is proved after the convergence of the observer. To highlight the efficiency and applicability of the proposed control scheme, simulation and experimental results are conducted for a 1.5kW induction motor.

Keywords: Backstepping control, fault detection and isolation, fault tolerant control, induction motors, second order sliding mode observers, sensorless control.

1. INTRODUCTION

Fault Tolerant Control (FTC) systems are able to maintain specific system performances not only under nominal conditions but also when faults occur. There are two types of FTC: active and passive approaches.

In the active approach, the overall design consists of two distinct steps. In the first step (Fault Detection and Isolation: FDI), a dynamical system (FDI block) is designed. By processing input/output data, the FDI block is able to detect the presence of an incipient fault and to isolate it from others faults or disturbances. In the second step (control reconfiguration step), the control law is changed according to the information provided by the FDI block, in order to compensate the effect of the faults and to maintain specific performances [1, 2]. Many FDI and online monitoring approaches have been suggested for linear and nonlinear systems: model-based techniques (observers [3], parity equations [4], parameters estimation [5], etc.), statistical techniques (principal component analysis, partial least squares [6, 7], etc.), artificial intelligent techniques (fuzzy logic [8], neural networks [8], etc).

In the passive approach [1, 2], a robust controller that can maintain acceptable performances against a set of faults is designed. This approach does not require the controller reconfiguration and the design of a FDI block.

Induction Motors (IM) are widely used in many indus-

trial processes due to their reliability, low cost and high performances. However, because of several stresses (mechanical, environmental, thermal, electrical), IM are subjected to various faults, such as stator short-circuits and rotor failures such as broken bars or rings, etc. Description of the different types of faults which can occur in the induction motors is given in [9]. Fault detection and isolation of IM have received considerable attention. Many FDI techniques have been applied such as model-based techniques using parameters estimation [10–13], signal processing techniques [14,15], artificial intelligence techniques [16], etc. In [11–13], the authors have studied the broken rotor bars faults in induction machines using parameters estimation approach. They have shown that in presence of broken rotor bars faults the rotor resistance increases.

In this paper, we design a passive fault tolerant controller for induction motors in order to compensate the load torque disturbance and the rotor resistance variations caused by broken rotor bars faults. The proposed approach consists of designing a robust controller which does not require a control reconfiguration and a FDI scheme.

In [17], a passive fault controller, which is able to compensate the rotor resistance variations and the effect of the load torque disturbance is proposed. The design approach uses a direct field oriented controller based on backstepping strategy to steer the flux and the speed to their desired references in presence of rotor resistance variations and load torque disturbance. Moreover, sensorless control is considered. This control method avoids the use of the speed sensor [18–21]. For instance, in [21], the feedback controller uses an adaptive observer in order to estimate the flux and the speed. In [20], the control scheme

Nadia Djeghali and Said Djennoune are with the Laboratoire de Conduite et Conception des Systèmes de Production, Université Mouloud MAMMERI de Tizi-Ouzou, B.P.17, 15000, Algérie (e-mail: {djeghali_nadya, s_djennoune}@yahoo.fr).

Malek Ghanes and Jean Pierre Barbot are with the ECS-Lab, ENSEA, France (e-mail: {ghanes, barbot}@ensea.fr).

is based on a first order sliding mode observer. The sliding mode observers are widely used due to their finite time convergence, robustness with respect to uncertainties and the possibility of uncertainty estimation [22, 23]. When we use the first order sliding mode approach, the chattering effect appears. To avoid the chattering effect, the high order sliding mode techniques have been developed. In [17], the controller uses a second order sliding mode observer [24–29] to estimate the speed and the flux. The second order sliding mode observer uses only the measured stator currents. The stability of the closed-loop system under the sliding mode observer is analyzed and the convergence of the closed-loop system trajectories to their respective desired values is proved. Finally, the efficiency of the proposed sensorless passive fault tolerant controller is validated by simulation where the speed and the load torque are taken constant.

In this work, the theoretical results established in [17] are taken up again for clarity. Moreover, the efficiency of the proposed controller is validated by both simulation and experimental results. Furthermore, the experimental and the simulation results are presented with complicated situations where the speed and the load torque are taken variable.

Compared to the existing fault tolerant control schemes already reported in the literature [30–33], the main contribution of the proposed approach is the combination of the backstepping control and the high order sliding mode observer to design a sensorless fault tolerant control for induction motors in presence of rotor resistance variation and load torque disturbance. The use of the high order sliding mode observers permits to avoid the chattering effect. Whereas the backstepping technique provides a simpler design procedure and it also avoids the chattering effect. This control technique does not force the designed system to appear linear, which can avoid cancellations of useful nonlinearities. Furthermore, additional nonlinear damping terms can be introduced in the feedback loop to enhance robustness. Another feature of backstepping designs is that the uncertainties which affect the system are not required to satisfy the matching condition. The second contribution of this work is the implementation of the proposed controller under complicated situations where the speed and the load torque are taken variable.

This paper is organized as follows: Section 2 describes the IM oriented model in presence of rotor resistance variations. Section 3 gives some definitions on practical stability and boundedness. Section 4 is devoted to the design of the robust backstepping controller which is able to steer the flux and speed variables to their desired references in presence of rotor resistance variations and load torque disturbance. In Section 5, a second order sliding mode observer is designed in order to estimate the flux and the speed. Section 6 studies the stability of the closed-loop system. In Section 7, simulation and experimental results

are obtained and demonstrate the efficiency and the applicability of the proposed approach. Section 8 gives some concluding remarks on the proposed controller.

2. INDUCTION MOTOR ORIENTED MODEL

In field oriented control, the flux vector is forced on the d-axis ($\phi_{qr} = \frac{d\phi_{qr}}{dt} = 0$). The resulting induction motor model in the $(d-q)$ reference frame is described by the following state equations [34]:

$$\begin{aligned}\frac{di_{ds}}{dt} &= -ai_{ds} + \omega_s i_{qs} + \frac{L_m}{\sigma L_s L_r \tau_r} \phi_{dr} + \frac{V_{ds}}{\sigma L_s} \\ \frac{di_{qs}}{dt} &= -ai_{qs} - \omega_s i_{ds} - \frac{L_m P}{\sigma L_s L_r} \Omega \phi_{dr} + \frac{V_{qs}}{\sigma L_s} \\ \frac{d\phi_{dr}}{dt} &= \frac{L_m}{\tau_r} i_{ds} - \frac{\phi_{dr}}{\tau_r} \\ \frac{d\Omega}{dt} &= \frac{PL_m}{L_r J} i_{qs} \phi_{dr} - \frac{f}{J} \Omega - \frac{T}{J}\end{aligned}\quad (1)$$

with:

$$\begin{aligned}\omega_s &= P\Omega + \frac{L_m}{\tau_r \phi_{dr}} i_{qs} \\ a &= \left(\frac{R_s}{\sigma L_s} + \frac{1-\sigma}{\sigma \tau_r} \right)\end{aligned}\quad (2)$$

Where σ is the coefficient of dispersion given by:

$$\sigma = 1 - \frac{L_m^2}{L_s L_r}$$

L_s, L_r, L_m are stator, rotor and mutual inductances, respectively. R_s, R_r are respectively stator and rotor resistances. ω_s is the stator pulsation. τ_r is the rotor time constant ($\tau_r = \frac{L_r}{R_r}$). P is the number of pole pairs. V_{ds}, V_{qs} are stator voltage components. ϕ_{dr}, ϕ_{qr} are the rotor flux components. Ω is the mechanical speed. T is the load torque. i_{ds}, i_{qs} are stator current components. J is the moment of inertia of the motor. f is the friction coefficient. Furthermore, an operating domain \mathcal{D} is defined by the following definition.

Definition 1: Operating domain \mathcal{D} : $I_{ds}^{max}, I_{qs}^{max}, \Phi_{dr}^{max}, \Omega^{max}$ and T^{max} are respectively the maximum values of the currents, flux, speed and the load torque such that $|i_{ds}| \leq I_{ds}^{max}, |i_{qs}| \leq I_{qs}^{max}, |\phi_{dr}| \leq \Phi_{dr}^{max}, |\Omega| \leq \Omega^{max}, |T| \leq T^{max}$.

2.1. Faulty model

Due to mechanical, environmental, thermal and electrical stresses, several faults can occur in the IM such as short-circuits in the stator, broken bars or rings in the rotor [9], etc. The considered faults here are broken rotor bars. These faults lead to the rotor resistance variations [11–13]. Let ΔR_r be the rotor resistance variation. Substituting R_r by $R_r + \Delta R_r$ in τ_r , then, in presence of ro-

tor resistance variations, the model (1) becomes [32]:

$$\begin{aligned}\frac{di_{ds}}{dt} &= -ai_{ds} + \omega_s i_{qs} + \frac{L_m}{\sigma L_s L_r \tau_r} \phi_{dr} + \frac{V_{ds}}{\sigma L_s} + h_1(x) \\ \frac{di_{qs}}{dt} &= -ai_{qs} - \omega_s i_{ds} - \frac{L_m P}{\sigma L_s L_r} \Omega \phi_{dr} + \frac{V_{qs}}{\sigma L_s} + h_2(x) \\ \frac{d\phi_{dr}}{dt} &= \frac{L_m}{\tau_r} i_{ds} - \frac{\phi_{dr}}{\tau_r} + h_3(x) \\ \frac{d\Omega}{dt} &= \frac{PL_m}{L_r J} i_{qs} \phi_{dr} - \frac{f}{J} \Omega - \frac{T}{J}\end{aligned}\quad (3)$$

where $x = [i_{ds} \ i_{qs} \ \phi_{dr} \ \Omega]^T$. $h_1(x)$, $h_2(x)$, $h_3(x)$ represent the fault terms due to rotor resistance variations, they are given by:

$$\begin{aligned}h_1(x) &= \Delta R_r \left(-\left(\frac{1-\sigma}{\sigma L_r}\right) i_{ds} + \frac{L_m}{\phi_{dr} L_r} i_{qs}^2 + \frac{L_m}{\sigma L_s L_r^2} \phi_{dr} \right) \\ h_2(x) &= \Delta R_r \left(-\left(\frac{1-\sigma}{\sigma L_r}\right) i_{qs} - \frac{L_m}{\phi_{dr} L_r} i_{ds} i_{qs} \right) \\ h_3(x) &= \Delta R_r \left(\frac{L_m}{L_r} i_{ds} - \frac{\phi_{dr}}{L_r} \right)\end{aligned}$$

2.2. Control objectives

Our control objective is to design a passive FTC to force the speed Ω and the flux ϕ_{dr} to track their desired references Ω^* and ϕ_{dr}^* , respectively with good tracking performance, under both load torque disturbance T and rotor resistance variations, which induces the term $h_i(x)$ in the model (3). The problem consists of designing a robust controller, which does not require control reconfiguration and FDI block. To achieve the above control objective, we use a direct field oriented controller based on the robust backstepping strategy. The closed loop performances can be achieved only if the the load torque disturbance T and the terms $h_i(x)$ induced by the rotor resistance variations are bounded and their bounds are known.

A further objective consists to avoid the use of a speed sensor. Hence, the controller is combined with a second order observer to achieve sensorless fault tolerant control. This observer eliminates the chattering effect. Other FTC methods which are not considered here are the active ones. In these methods, first, a FDI block detects and isolates the fault and, second, the control law is changed according to the information provided by the FDI block [1, 2].

3. PRELIMINARIES

Here we introduce some definitions on the practical stability and boundedness which will be used in next sections [35, 36]. Consider the following system:

$$\begin{aligned}\dot{x} &= f(t, x) \\ x(t_0) &= x_0, \ t_0 \geq 0\end{aligned}\quad (4)$$

where $x \in R^n$ is the state, $t \in R_{\geq 0}$ is the time and $f : R_{\geq 0} \times R^n \rightarrow R^n$ is piecewise continuous in t and locally Lipschitz in x . (t_0, x_0) are the initial conditions. We recall the following definition of practical stability of (4). Let B_r denotes the closed loop ball in R^n of radius $r > 0$, i.e. : $B_r = \{x \in R^n : \|x\| \leq r\}$, with $\|\cdot\|$ denotes the Euclidean norm of vectors.

Definition 2: [36] The system (4) is said to be globally uniformly exponentially practically stable (or convergent to a ball B_r with radius $r > 0$), if there exist $\beta > 0$ and $k \geq 0$, such that for all $t_0 \in R_{\geq 0}$ and all $x_0 \in R^n$,

$$\|x\| \leq k\|x_0\| \exp(-\beta(t-t_0)) + r, \ \forall t \geq t_0 \quad (5)$$

Theorem 1: [36] Consider system (4). Let $V(t, x) : R_{\geq 0} \times R^n \rightarrow R$ be a continuously differentiable function such that

$$c_1 \|x\|^2 \leq V(t, x) \leq c_2 \|x\|^2 + a_1, \quad (6)$$

$$\frac{\partial V}{\partial t} + \frac{\partial V}{\partial x}(f(t, x)) \leq -c_3 V(t, x) + \rho_1, \quad (7)$$

$$\left\| \frac{\partial V}{\partial x} \right\| \leq c_4 \|x\| + b_1. \quad (8)$$

for all $t_0 \in R_{\geq 0}$ and all $x \in R^n$, where $c_1, c_2, c_3, c_4, \rho_1, a_1$ and b_1 are positive constants. Then, system (4) is globally uniformly exponentially practically stable.

To study the boundedness of the system (4) we use the following definition.

Definition 3: [35] The system (4) is globally uniformly bounded, if there exists a continuous positive definite function $W_3(x)$ such that the derivative of the Lyapunov function V along the trajectories of the system (4) satisfies:

$$\dot{V} \leq -W_3(x), \ \forall \|x\| \geq \mu > 0, \ \forall t \geq t_0 \quad (9)$$

i.e for every $a > 0$ there exists $b = b(a) > 0$ such that, for all $t_0 \geq 0$,

$$\|x(t_0)\| \leq a \Rightarrow \|x(t)\| \leq b(a), \ \forall t \geq t_0 \quad (10)$$

4. BACKSTEPPING CONTROL DESIGN

This part deals with the speed and flux control by means of the robust backstepping control. The idea of backstepping design is to select recursively some appropriate functions of state variables as virtual control inputs for lower dimension subsystems of the overall system. At each step of the backstepping, a new virtual control input is designed. When the procedure terminates, the actual control input results which achieves the original design objective by virtue of a final Lyapunov function, which is formed by summing up the Lyapunov functions associated with each individual design step. An overview on the various backstepping design techniques, including integrator backstepping, backstepping for strict-feedback systems, adaptive

backstepping and robust backstepping is given in [37]. In this work, in order to compensate the rotor resistance variations and the load disturbance, the robust backstepping technique is used. In this control technique, the control law (stabilizing function) in each step uses the *sign* function in order to compensate the uncertainties. Since the stabilizing function is required to be continuously differentiable, the *sign* function is approximated by the hyperbolic function *tanh*. The following lemma quantifies the approximation error of a *sign* function by an hyperbolic function *tanh* [38].

Lemma 1: Given any $\varepsilon > 0$, the following inequality holds

$$0 \leq k.x.sign(x) - k.x.tanh\left(\frac{kh}{\varepsilon}x\right) \leq \varepsilon \quad (11)$$

where x is the state variable, $h = 0.2785$ and k is any positive number. The proof of this lemma can be found in [38].

Assumptions 1: a- All states variables i_{ds} , i_{qs} , ϕ_{dr} and Ω are bounded and remain in the operating domain \mathcal{D} for all $t \geq 0$.

b- The desired trajectories of the flux and the speed (ϕ_{dr}^* and Ω^*) are in the operating domain \mathcal{D} .

c- The actual load torque is assumed to be bounded by a maximal fixed value T_{max} . This maximal value is chosen in accordance to the realistic torque characteristics of the chosen drive $|T| \leq T^{max}$.

From assumptions 1 and by the fact that the rotor resistance variation ΔR_r is finite, then the function $h_i(x) : R^4 \rightarrow R$, $i = \overline{1,3}$ are bounded in \mathcal{D} , that is $|h_i(x)| \leq H_i^{max}$, $i = \overline{1,3}$.

4.1. Step1: Flux control

The objective is to steer the flux ϕ_{dr} to a desired reference ϕ_{dr}^* , let $e_\phi = \phi_{dr} - \phi_{dr}^*$ be the flux tracking error. The dynamic of e_ϕ is:

$$\dot{e}_\phi = \frac{L_m}{\tau_r} i_{ds} - \frac{\phi_{dr}}{\tau_r} + h_3(x) - \dot{\phi}_{dr}^* \quad (12)$$

A Lyapunov function is defined as:

$$V_\phi = \frac{1}{2} e_\phi^2 \quad (13)$$

By deriving (13) we obtain:

$$\dot{V}_\phi = e_\phi \dot{e}_\phi = e_\phi \left(\frac{L_m}{\tau_r} i_{ds} - \frac{\phi_{dr}}{\tau_r} + h_3(x) - \dot{\phi}_{dr}^* \right) \quad (14)$$

To make \dot{V}_ϕ negative definite, i_{ds} is chosen as virtual element of control for stabilizing the flux, its desired value i_{ds}^* is defined as:

$$i_{ds}^* = \frac{\tau_r}{L_m} \left(-k_\phi e_\phi - k_1 \tanh\left(\frac{k_1 h}{\varepsilon_1} e_\phi\right) + \frac{\phi_{dr}}{\tau_r} + \dot{\phi}_{dr}^* \right) \quad (15)$$

where $h = 0.2785$ (see Lemma 1). k_1 , k_ϕ and ε_1 are positive design parameters.

By setting $i_{ds} = i_{ds}^*$ in (14) we get :

$$\dot{V}_\phi = -k_\phi e_\phi^2 - k_1 \tanh\left(\frac{k_1 h}{\varepsilon_1} e_\phi\right) e_\phi + h_3(x) e_\phi \quad (16)$$

for $k_1 \geq H_3^{max}$ we get:

$$\dot{V}_\phi \leq -k_\phi e_\phi^2 - k_1 \tanh\left(\frac{k_1 h}{\varepsilon_1} e_\phi\right) e_\phi + k_1 |e_\phi| \quad (17)$$

with:

$$|e_\phi| = e_\phi \text{sign}(e_\phi) \quad (18)$$

The derivative of the Lyapunov function (17) becomes:

$$\dot{V}_\phi \leq -k_\phi e_\phi^2 - k_1 \tanh\left(\frac{k_1 h}{\varepsilon_1} e_\phi\right) e_\phi + k_1 e_\phi \text{sign}(e_\phi) \quad (19)$$

we have (see Lemma 1):

$$0 \leq k_1 e_\phi \text{sign}(e_\phi) - k_1 \tanh\left(\frac{k_1 h}{\varepsilon_1} e_\phi\right) e_\phi \leq \varepsilon_1 \quad (20)$$

The derivative of the Lyapunov function (19) becomes:

$$\dot{V}_\phi \leq -k_\phi e_\phi^2 + \varepsilon_1 \quad (21)$$

Also, we have:

$$\left| \frac{\partial V_\phi}{\partial e_\phi} \right| = |e_\phi| \leq |e_\phi| + b_\phi \quad \forall b_\phi > 0 \quad (22)$$

Following Theorem 1, the inequalities (21) and (22) imply that the variable e_ϕ is globally uniformly exponentially practically stable (e_ϕ converges to a ball whose radius can be reduced by making small the tuning parameter ε_1).

4.2. Step2: Speed control

The objective is to steer the speed Ω to the desired reference Ω^* , let $e_\Omega = \Omega - \Omega^*$ be the speed tracking error. The error dynamic of the speed is:

$$\dot{e}_\Omega = \frac{PL_m}{L_r J} i_{qs} \phi_{dr} - \frac{f}{J} \Omega - \frac{T}{J} - \dot{\Omega}^* \quad (23)$$

A Lyapunov function is defined as:

$$V_\Omega = \frac{1}{2} e_\Omega^2 \quad (24)$$

By deriving (24) we obtain:

$$\dot{V}_\Omega = e_\Omega \dot{e}_\Omega = e_\Omega \left(\frac{PL_m}{L_r J} i_{qs} \phi_{dr} - \frac{f}{J} \Omega - \frac{T}{J} - \dot{\Omega}^* \right) \quad (25)$$

i_{qs} is chosen as virtual element of control for stabilizing the speed, its desired value i_{qs}^* is defined as:

$$i_{qs}^* = \frac{J L_r}{L_m P \phi_{dr}} \left(-k_\Omega e_\Omega - k_2 \tanh\left(\frac{k_2 h}{\varepsilon_2} e_\Omega\right) + \frac{f}{J} \Omega + \dot{\Omega}^* \right), \quad \phi_{dr} \neq 0 \quad (26)$$

where k_2 and k_Ω and ε_2 are positive design parameters. By setting $i_{qs} = i_{qs}^*$ in (25) we get:

$$\dot{V}_\Omega = e_\Omega(-k_\Omega e_\Omega - k_2 \tanh(\frac{k_2 h}{\varepsilon_2} e_\Omega) - \frac{T}{J}) \quad (27)$$

In the operating domain defined in Definition 1, the load torque T is assumed bounded, that is $|T| \leq T^{max}$. In order to make the controller robust against the load torque disturbance T , k_2 must be chosen as follows: $k_2 \geq \frac{T^{max}}{J}$. Then we obtain:

$$\dot{V}_\Omega \leq -k_\Omega e_\Omega^2 - k_2 \tanh(\frac{k_2 h}{\varepsilon_2} e_\Omega) e_\Omega + k_2 |e_\Omega| \leq -k_\Omega e_\Omega^2 + \varepsilon_2 \quad (28)$$

Moreover, we have:

$$\left| \frac{\partial V_\Omega}{\partial e_\Omega} \right| = |e_\Omega| \leq |e_\Omega| + b_\Omega \quad \forall b_\Omega > 0 \quad (29)$$

By Theorem 1, the inequalities (28) and (29) imply that the variable e_Ω is globally uniformly exponentially practically stable (e_Ω converges to a ball whose radius can be reduced by making small the tuning parameter ε_2).

4.3. Step3: Currents control

The objective is to steer the currents i_{ds} and i_{qs} to their desired references i_{ds}^* and i_{qs}^* , respectively. Let $e_d = i_{ds} - i_{ds}^*$ and $e_q = i_{qs} - i_{qs}^*$ be the tracking errors of the currents, then the dynamics of the tracking errors are:

$$\begin{aligned} \dot{e}_d &= -a i_{ds} + \omega_s i_{qs} + \frac{L_m}{\sigma L_s L_r \tau_r} \phi_{dr} + \frac{V_{ds}}{\sigma L_s} \\ &\quad - \frac{\tau_r}{L_m} F_1(e_\phi) \left(\frac{L_m}{\tau_r} i_{ds} - \frac{\phi_{dr}}{\tau_r} \right) - \frac{\tau_r}{L_m} \ddot{\phi}_{dr}^* \\ &\quad + \frac{\tau_r}{L_m} \left(F_1(e_\phi) - \frac{1}{\tau_r} \right) \dot{\phi}_{dr} + h_1(x) - \frac{\tau_r}{L_m} F_1(e_\phi) h_3(x) \\ \dot{e}_q &= -a i_{qs} - \omega_s i_{ds} - \frac{L_m}{\sigma L_s L_r} P \Omega \phi_{dr} + \frac{V_{qs}}{\sigma L_s} \\ &\quad - F_3(e_\Omega, \Omega, \phi_{dr}) - \frac{J L_r}{L_m P \phi_{dr}} \ddot{\Omega}^* \\ &\quad - \frac{J L_r}{L_m P \phi_{dr}} F_2(e_\Omega) \left(\frac{P L_m}{L_r J} i_{qs} \phi_{dr} - \frac{f}{J} \Omega \right) \\ &\quad - \frac{J L_r}{L_m P \phi_{dr}} \left(\frac{f}{J} - F_2(e_\Omega) \right) \dot{\Omega}^* \\ &\quad + h_2(x) + \frac{L_r F_2(e_\Omega)}{P L_m \phi_{dr}} T - F_4 h_3(x) \\ \dot{e}_\phi &= -k_\phi e_\phi - k_1 \tanh(\frac{k_1 h}{\varepsilon_1} e_\phi) + \frac{L_m}{\tau_r} e_d + h_3(x) \\ \dot{e}_\Omega &= \frac{P L_m}{L_r J} e_q \phi_{dr} - k_\Omega e_\Omega - k_2 \tanh(\frac{k_2 h}{\varepsilon_2} e_\Omega) - \frac{T}{J} \end{aligned} \quad (30)$$

where:

$$F_1(e_\phi) = -k_\phi - \frac{k_1^2 h}{\varepsilon_1} \left(1 - \tanh(\frac{k_1 h}{\varepsilon_1} e_\phi)^2 \right) + \frac{1}{\tau_r}$$

$$F_2(e_\Omega) = -k_\Omega - \frac{k_2^2 h}{\varepsilon_2} \left(1 - \tanh(\frac{k_2 h}{\varepsilon_2} e_\Omega)^2 \right) + \frac{f}{J}$$

$$F_3(e_\Omega, \Omega, \phi_{dr}) = \left(\frac{L_m}{\tau_r} i_{ds} - \frac{\phi_{dr}}{\tau_r} \right) F_4(e_\Omega, \Omega, \phi_{dr})$$

$$F_4(e_\Omega, \Omega, \phi_{dr}) = \frac{J L_r}{P L_m \phi_{dr}^2} \left(k_\Omega e_\Omega + k_2 \tanh(\frac{k_2 h}{\varepsilon_2} e_\Omega) - \frac{f}{J} \Omega - \dot{\Omega}^* \right)$$

The actual control inputs are chosen as follows:

$$\begin{aligned} V_{ds} &= \sigma L_s \left(-k_d e_d - k_3 \tanh\left(\frac{k_3 h}{\varepsilon_3} e_d\right) + a i_{ds} - \frac{L_m}{\tau_r} e_\phi \right. \\ &\quad \left. - \omega_s i_{qs} - \frac{L_m}{\sigma L_s L_r \tau_r} \phi_{dr} + \frac{\tau_r}{L_m} F_1\left(\frac{L_m}{\tau_r} i_{ds} - \frac{\phi_{dr}}{\tau_r}\right) \right. \\ &\quad \left. - \frac{\tau_r}{L_m} \left(F_1 - \frac{1}{\tau_r} \right) \dot{\phi}_{dr}^* + \frac{\tau_r}{L_m} \ddot{\phi}_{dr}^* \right) \end{aligned} \quad (31)$$

$$\begin{aligned} V_{qs} &= \sigma L_s \left(-k_q e_q - k_4 \tanh\left(\frac{k_4 h}{\varepsilon_4} e_q\right) + a i_{qs} + \omega_s i_{ds} \right. \\ &\quad \left. + \frac{L_m}{\sigma L_s L_r} P \Omega \phi_{dr} - \frac{P L_m}{J L_r} e_\Omega \phi_{dr} + F_3(e_\Omega, \Omega, \phi_{dr}) \right. \\ &\quad \left. + \frac{J L_r}{L_m P \phi_{dr}} F_2(e_\Omega) \left(\frac{P L_m}{L_r J} i_{qs} \phi_{dr} - \frac{f}{J} \Omega \right) \right. \\ &\quad \left. + \frac{J L_r}{L_m P \phi_{dr}} \left(\frac{f}{J} - F_2(e_\Omega) \right) \dot{\Omega}^* + \frac{J L_r}{L_m P \phi_{dr}} \ddot{\Omega}^* \right) \end{aligned} \quad (32)$$

Since the functions $h_i(x)$, $i = \overline{1, 3}$ and T are assumed to be bounded in \mathcal{D} , then the terms $(h_1(x) - \frac{\tau_r}{L_m} F_1(e_\phi) h_3(x))$ and $(h_2(x) - F_4 h_3(x) + \frac{L_r F_2(e_\Omega)}{P L_m \phi_{dr}} T)$ are also bounded in \mathcal{D} that is:

$$\left| h_1(x) - \frac{\tau_r}{L_m} F_1(e_\phi) h_3(x) \right| \leq G_1^{max}$$

$$\left| h_2(x) - F_4 h_3(x) + \frac{L_r F_2(e_\Omega)}{P L_m \phi_{dr}} T \right| \leq G_2^{max}$$

Proposition 1: Let k_d , k_q , k_1 , k_2 , k_3 and k_4 be positive design parameters and let ε_1 , ε_2 , ε_3 and ε_4 be arbitrary positive small parameters. If $k_1 \geq H_3^{max}$, $k_2 \geq \frac{T^{max}}{J}$, $k_3 \geq G_1^{max}$ and $k_4 \geq G_2^{max}$, then the dynamical system of tracking errors (30), driven by the control inputs (31) and (32), is globally uniformly exponentially practically stable.

Proof: The proof consists in showing that the errors variables e_ϕ , e_Ω , e_d and e_q in the system (30) driven by the control inputs V_{ds} and V_{qs} given by (31) and (32) respectively, are globally uniformly exponentially practically sta-

ble. By substituting (31) and (32) in (30) we get:

$$\begin{aligned}
\dot{e}_d &= -k_d e_d - k_3 \tanh\left(\frac{k_3 h}{\varepsilon_3} e_d\right) - \frac{L_m}{\tau_r} e_\phi + h_1(x) \\
&\quad - \frac{\tau_r}{L_m} F_1 h_3(x) \\
\dot{e}_q &= -k_q e_q - k_4 \tanh\left(\frac{k_4 h}{\varepsilon_4} e_q\right) - \frac{PL_m}{JL_r} e_\Omega \phi_{dr} + h_2(x) \\
&\quad - F_4 h_3(x) + \frac{L_r F_2(e_\Omega)}{PL_m \phi_{dr}} T \\
\dot{e}_\phi &= -k_\phi e_\phi - k_1 \tanh\left(\frac{k_1 h}{\varepsilon_1} e_\phi\right) + \frac{L_m}{\tau_r} e_d + h_3(x) \\
\dot{e}_\Omega &= \frac{PL_m}{L_r J} e_q \phi_{dr} - k_\Omega e_\Omega - k_2 \tanh\left(\frac{k_2 h}{\varepsilon_2} e_\Omega\right) - \frac{T}{J}
\end{aligned} \tag{33}$$

Consider the following Lyapunov function:

$$V = \frac{1}{2}(e_d^2 + e_q^2 + e_\phi^2 + e_\Omega^2) = \frac{1}{2} \|e\|^2 \tag{34}$$

where $e = [e_d \ e_q \ e_\phi \ e_\Omega]^T$. From the steps 1 and 2, we have $k_1 \geq H_3^{max}$ and $k_2 \geq \frac{T^{max}}{J}$. Then, for $k_3 \geq G_1^{max}$ and $k_4 \geq G_2^{max}$, we get:

$$\dot{V} \leq -k_\phi e_\phi^2 - k_\Omega e_\Omega^2 - k_d e_d^2 - k_q e_q^2 + \varepsilon_1 + \varepsilon_2 + \varepsilon_3 + \varepsilon_4 \tag{35}$$

Let $c_3 = 2\max\{k_\phi, k_\Omega, k_d, k_q\}$ and $\rho_e = \varepsilon_1 + \varepsilon_2 + \varepsilon_3 + \varepsilon_4$, then (35) becomes:

$$\dot{V} \leq -c_3 V + \rho_e \tag{36}$$

In addition, we have:

$$\left\| \frac{\partial V}{\partial e} \right\| = \|e\| \leq \|e\| + b \quad \forall b > 0 \tag{37}$$

By Theorem 1, the inequalities (36) and (37) imply that the error variables e_ϕ , e_Ω , e_d and e_q converge to a ball whose radius can be reduced by making small the tuning parameters ε_i , $i = \overline{1, 4}$. This means that the error variables are globally uniformly exponentially practically stable. \square

5. SECOND ORDER SLIDING MODE OBSERVER DESIGN

In order to implement the control laws (31) and (32) without flux and speed sensors, a second order sliding mode observer [24–29] is used to estimate the speed Ω and the flux ϕ_{dr} . The IM model in $(\alpha - \beta)$ reference frame is

given by:

$$\begin{aligned}
\dot{i}_{\alpha s} &= -a i_{\alpha s} + \frac{L_m}{\sigma L_s L_r \tau_r} \phi_{\alpha r} + \frac{L_m P}{\sigma L_s L_r} \Omega \phi_{\beta r} + \frac{V_{\alpha s}}{\sigma L_s} \\
\dot{i}_{\beta s} &= -a i_{\beta s} - \frac{L_m P}{\sigma L_s L_r} \Omega \phi_{\alpha r} + \frac{L_m}{\sigma L_s L_r \tau_r} \phi_{\beta r} + \frac{V_{\beta s}}{\sigma L_s} \\
\dot{\phi}_{\alpha r} &= -P \Omega \phi_{\beta r} + \frac{L_m}{\tau_r} i_{\alpha s} - \frac{1}{\tau_r} \phi_{\alpha r} \\
\dot{\phi}_{\beta r} &= P \Omega \phi_{\alpha r} + \frac{L_m}{\tau_r} i_{\beta s} - \frac{1}{\tau_r} \phi_{\beta r} \\
\dot{\Omega} &= \frac{PL_m}{L_r J} (i_{\beta s} \phi_{\alpha r} - i_{\alpha s} \phi_{\beta r}) - \frac{f}{J} \Omega - \frac{T}{J}
\end{aligned} \tag{38}$$

with $i_{\alpha s}, i_{\beta s}$ are the stator current components, they are assumed to be measured. $\phi_{\alpha r}, \phi_{\beta r}$ are the rotor flux components. Ω is the mechanical speed. T is the load torque. $V_{\alpha s}$ and $V_{\beta s}$ are the stator voltage components given by:

$$V_{\alpha s} = \cos(\rho) V_{ds} - \sin(\rho) V_{qs}$$

$$V_{\beta s} = \sin(\rho) V_{ds} + \cos(\rho) V_{qs}$$

with $\rho = \arctan \frac{\phi_{\beta r}}{\phi_{\alpha r}}$.

By applying the following change of variables:

$$\begin{aligned}
z_1 &= i_{\alpha s} \\
z_2 &= i_{\beta s} \\
z_3 &= \frac{L_m}{\sigma L_s L_r \tau_r} \phi_{\alpha r} + \frac{L_m P}{\sigma L_s L_r} \Omega \phi_{\beta r} \\
z_4 &= -\frac{L_m P}{\sigma L_s L_r} \Omega \phi_{\alpha r} + \frac{L_m}{\sigma L_s L_r \tau_r} \phi_{\beta r} \\
z_5 &= \dot{z}_3 \\
z_6 &= \dot{z}_4
\end{aligned} \tag{39}$$

The system (38) becomes as follows:

$$\begin{aligned}
\dot{z}_1 &= -a z_1 + z_3 + \frac{V_{\alpha s}}{\sigma L_s} \\
\dot{z}_2 &= -a z_2 + z_4 + \frac{V_{\beta s}}{\sigma L_s} \\
\dot{z}_3 &= z_5 \\
\dot{z}_4 &= z_6 \\
\dot{z}_5 &= z_7 \\
\dot{z}_6 &= z_8
\end{aligned} \tag{40}$$

A second order sliding mode observer is defined as [29]:

$$\begin{aligned}
\dot{\hat{z}}_1 &= -a z_1 + \tilde{z}_3 + \lambda_1 |z_1 - \hat{z}_1|^{0.5} \text{sign}(z_1 - \hat{z}_1) + \frac{V_{\alpha s}}{\sigma L_s} \\
\dot{\hat{z}}_3 &= \alpha_1 \text{sign}(z_1 - \hat{z}_1) \\
\dot{\hat{z}}_2 &= -a z_2 + \tilde{z}_4 + \lambda_2 |z_2 - \hat{z}_2|^{0.5} \text{sign}(z_2 - \hat{z}_2) + \frac{V_{\beta s}}{\sigma L_s} \\
\dot{\hat{z}}_4 &= \alpha_2 \text{sign}(z_2 - \hat{z}_2) \\
\dot{\hat{z}}_3 &= E_1 E_2 \left(\tilde{z}_5 + \lambda_3 |\tilde{z}_3 - \hat{z}_3|^{0.5} \text{sign}(\tilde{z}_3 - \hat{z}_3) \right) \\
\dot{\hat{z}}_5 &= E_1 E_2 \alpha_3 \text{sign}(\tilde{z}_3 - \hat{z}_3) \\
\dot{\hat{z}}_4 &= E_1 E_2 \left(\tilde{z}_6 + \lambda_4 |\tilde{z}_4 - \hat{z}_4|^{0.5} \text{sign}(\tilde{z}_4 - \hat{z}_4) \right) \\
\dot{\hat{z}}_6 &= E_1 E_2 \alpha_4 \text{sign}(\tilde{z}_4 - \hat{z}_4) \\
\dot{\hat{z}}_5 &= E_1 E_2 E_3 E_4 \left(\tilde{z}_7 + \lambda_5 |\tilde{z}_5 - \hat{z}_5|^{0.5} \text{sign}(\tilde{z}_5 - \hat{z}_5) \right) \\
\dot{\hat{z}}_7 &= E_1 E_2 E_3 E_4 \alpha_5 \text{sign}(\tilde{z}_5 - \hat{z}_5) \\
\dot{\hat{z}}_6 &= E_1 E_2 E_3 E_4 \left(\tilde{z}_8 + \lambda_6 |\tilde{z}_6 - \hat{z}_6|^{0.5} \text{sign}(\tilde{z}_6 - \hat{z}_6) \right) \\
\dot{\hat{z}}_8 &= E_1 E_2 E_3 E_4 \alpha_6 \text{sign}(\tilde{z}_6 - \hat{z}_6)
\end{aligned} \tag{41}$$

where $E_i = 1$ if $\tilde{z}_i - \hat{z}_i = 0$ else $E_i = 0$ for $i=1, \dots, n$. with $\tilde{z}_1 = z_1$, $\tilde{z}_2 = z_2$. For a suitable choice of the parameters λ_i and α_i : $\alpha_i > z_{(i+4)\max}$, $\lambda_i > (\alpha_i + z_{(i+4)\max}) \sqrt{\frac{2}{\alpha_i - z_{(i+4)\max}}}$, $i = 1, \dots, n$, the observation errors ($\tilde{z}_i - \hat{z}_i$) tend to zero in finite time [24, 27, 29]). Then, the speed and the flux are estimated as follows:

From equations (39) we have:

$$\begin{aligned}
z_3 &= b \phi_{\alpha r} + c \Omega \phi_{\beta r} \\
z_4 &= -c \Omega \phi_{\alpha r} + b \phi_{\beta r}
\end{aligned} \tag{42}$$

where: $b = \frac{L_m}{\sigma L_s L_r \tau_r}$, $c = \frac{L_m P}{\sigma L_s L_r}$.
By solving the above equations we get:

$$\phi_{\alpha r} = \frac{b z_3 - c \Omega z_4}{b^2 + c^2 \Omega^2}, \quad \phi_{\beta r} = \frac{c \Omega z_3 + b z_4}{b^2 + c^2 \Omega^2}$$

Substituting z_3 and z_4 by their estimates \hat{z}_3 and \hat{z}_4 we obtain the flux estimates as follows:

$$\hat{\phi}_{\alpha r} = \frac{b \hat{z}_3 - c \hat{\Omega} \hat{z}_4}{b^2 + c^2 \hat{\Omega}^2}, \quad \hat{\phi}_{\beta r} = \frac{c \hat{\Omega} \hat{z}_3 + b \hat{z}_4}{b^2 + c^2 \hat{\Omega}^2}$$

By deriving the equations (42) we get:

$$z_5 = \dot{z}_3 = -\frac{1}{\tau_r} z_3 - P \Omega z_4 + b \frac{L_m}{\tau_r} i_{\alpha s} + c \frac{L_m}{\tau_r} \Omega i_{\beta s} + c \phi_{\beta r} \dot{\Omega} \tag{43}$$

$$z_6 = \dot{z}_4 = -\frac{1}{\tau_r} z_4 + P \Omega z_3 + b \frac{L_m}{\tau_r} i_{\beta s} - c \frac{L_m}{\tau_r} \Omega i_{\alpha s} - c \phi_{\alpha r} \dot{\Omega} \tag{44}$$

The estimate of the speed $\hat{\Omega}$ and its derivative $\dot{\hat{\Omega}}$ can be obtained from (43) and (44), where the variables z_3 , z_4 , z_5 , z_6 , $\phi_{\alpha r}$ and $\phi_{\beta r}$ must be replaced by their estimates \hat{z}_3 ,

\hat{z}_4 , \hat{z}_5 , \hat{z}_6 , $\hat{\phi}_{\alpha r}$ and $\hat{\phi}_{\beta r}$, respectively.

In the $(d-q)$ reference frame the estimated flux and currents are given as follows:

$$\hat{i}_{ds} = \cos(\hat{\rho}) i_{\alpha s} + \sin(\hat{\rho}) i_{\beta s}$$

$$\hat{i}_{qs} = -\sin(\hat{\rho}) i_{\alpha s} + \cos(\hat{\rho}) i_{\beta s}$$

$$\hat{\rho} = \arctan \frac{\hat{\phi}_{\beta r}}{\hat{\phi}_{\alpha r}}, \quad \hat{\phi}_{dr} = \sqrt{\hat{\phi}_{\alpha r}^2 + \hat{\phi}_{\beta r}^2}$$

Since the sliding mode observer converges in finite time, then there exists $t_s > 0$ such that $\hat{i}_{ds}(t) = i_{ds}(t)$, $\hat{i}_{qs}(t) = i_{qs}(t)$, $\hat{\phi}_{dr}(t) = \phi_{dr}(t)$ and $\hat{\Omega}(t) = \Omega(t)$ for all $t \geq t_s$.

6. STABILITY ANALYSIS OF THE CLOSED-LOOP SYSTEM

To implement the control laws (31) and (32), the speed and the flux and the currents must be replaced by their estimates as follows:

$$\begin{aligned}
V_{ds} &= \sigma L_s \left(-k_d \hat{e}_d - k_3 \tanh \left(\frac{k_3 h}{\varepsilon_3} \hat{e}_d \right) + a \hat{i}_{ds} - \frac{L_m}{\tau_r} \hat{e}_\phi \right. \\
&\quad \left. - \hat{\omega}_s \hat{i}_{qs} - \frac{L_m}{\sigma L_s L_r \tau_r} \hat{\phi}_{dr} + \frac{\tau_r}{L_m} F_1(\hat{e}_\phi) \left(\frac{L_m}{\tau_r} \hat{i}_{ds} - \frac{\hat{\phi}_{dr}}{\tau_r} \right) \right. \\
&\quad \left. - \frac{\tau_r}{L_m} \left(F_1(\hat{e}_\phi) - \frac{1}{\tau_r} \right) \hat{\phi}_{dr}^* + \frac{\tau_r}{L_m} \hat{\phi}_{dr}^* \right)
\end{aligned} \tag{45}$$

$$\begin{aligned}
V_{qs} &= \sigma L_s \left(-k_q \hat{e}_q - k_4 \tanh \left(\frac{k_4 h}{\varepsilon_4} \hat{e}_q \right) + a \hat{i}_{qs} + \hat{\omega}_s \hat{i}_{ds} \right. \\
&\quad \left. + \frac{L_m}{\sigma L_s L_r} P \hat{\Omega} \hat{\phi}_{dr} - \frac{P L_m}{J L_r} \hat{e}_\Omega \hat{\phi}_{dr} + F_3(\hat{e}_\Omega, \hat{\Omega}, \hat{\phi}_{dr}) \right. \\
&\quad \left. + \frac{J L_r}{L_m P \hat{\phi}_{dr}} F_2(\hat{e}_\Omega) \left(\frac{P L_m}{L_r J} \hat{i}_{qs} \hat{\phi}_{dr} - \frac{f}{J} \hat{\Omega} \right) \right. \\
&\quad \left. + \frac{J L_r}{L_m P \hat{\phi}_{dr}} \left(\frac{f}{J} - F_2(\hat{e}_\Omega) \right) \dot{\hat{\Omega}}^* + \frac{J L_r}{L_m P \hat{\phi}_{dr}} \ddot{\hat{\Omega}}^* \right)
\end{aligned} \tag{46}$$

where: $\hat{e}_d = \hat{i}_{ds} - \hat{i}_{ds}^*$, $\hat{e}_q = \hat{i}_{qs} - \hat{i}_{qs}^*$, $\hat{e}_\Omega = \hat{\Omega} - \Omega^*$, $\hat{e}_\phi = \hat{\phi}_{dr} - \phi_{dr}^*$, $\hat{\omega}_s = P \hat{\Omega} + \frac{L_m}{\tau_r \phi_{dr}} \hat{i}_{qs}$.

$$\hat{i}_{ds}^* = \frac{\tau_r}{L_m} \left(-k_\phi \hat{e}_\phi - k_1 \tanh \left(\frac{k_1 h}{\varepsilon_1} \hat{e}_\phi \right) + \frac{\hat{\phi}_{dr}}{\tau_r} + \hat{\phi}_{dr}^* \right)$$

$$\hat{i}_{qs}^* = \frac{J L_r}{L_m P \hat{\phi}_{dr}} \left(-k_\Omega \hat{e}_\Omega - k_2 \tanh \left(\frac{k_2 h}{\varepsilon_2} \hat{e}_\Omega \right) + \frac{f}{J} \hat{\Omega} + \dot{\hat{\Omega}}^* \right)$$

By substituting the control laws (45) and (46) in the

system of the tracking errors (30) we get:

$$\begin{aligned}
\dot{e}_d &= -k_d e_d - k_3 \tanh\left(\frac{k_3 h}{\varepsilon_3}(e_d + \varepsilon_d + i_{ds}^* - \hat{i}_{ds}^*)\right) - \frac{L_m}{\tau_r} e_\phi \\
&\quad + h_1(x) - \frac{\tau_r}{L_m} F_1(e_\phi) h_3(x) + d_1(\varepsilon, x, \hat{x}) \\
\dot{e}_q &= -k_q e_q - k_4 \tanh\left(\frac{k_4 h}{\varepsilon_4}(e_q + \varepsilon_q + i_{qs}^* - \hat{i}_{qs}^*)\right) \\
&\quad - \frac{PL_m}{JL_r} \phi_{dr} e_\Omega + h_2(x) + \frac{L_r F_2(e_\Omega)}{PL_m \phi_{dr}} T - F_4 h_3(x) \\
&\quad + d_2(\varepsilon, x, \hat{x}) \\
\dot{e}_\phi &= -k_\phi e_\phi - k_1 \tanh\left(\frac{k_1 h}{\varepsilon_1} e_\phi\right) + \frac{L_m}{\tau_r} e_d + h_3(x) \\
\dot{e}_\Omega &= \frac{PL_m}{L_r J} e_q \phi_{dr} - k_\Omega e_\Omega - k_2 \tanh\left(\frac{k_2 h}{\varepsilon_2} e_\Omega\right) - \frac{T}{J}
\end{aligned} \tag{47}$$

with: $\varepsilon = [\varepsilon_d \ \varepsilon_q \ \varepsilon_\phi \ \varepsilon_\Omega]^T$ denotes the vector of the estimation errors where: $\varepsilon_d = i_{ds} - \hat{i}_{ds}$, $\varepsilon_q = i_{qs} - \hat{i}_{qs}$, $\varepsilon_\phi = \phi_{dr} - \hat{\phi}_{dr}$, $\varepsilon_\Omega = \Omega - \hat{\Omega}$. $x = [i_{ds} \ i_{qs} \ \phi_{dr} \ \Omega]^T$, $\hat{x} = [\hat{i}_{ds} \ \hat{i}_{qs} \ \hat{\phi}_{dr} \ \hat{\Omega}]^T$. The perturbation terms $d_1(\varepsilon, x, \hat{x})$ and $d_2(\varepsilon, x, \hat{x})$ are due to the presence of the observer, they are given by:

$$\begin{aligned}
d_1(\varepsilon, x, \hat{x}) &= -(k_d + a)\varepsilon_d - k_d(i_{ds}^* - \hat{i}_{ds}^*) + \frac{L_m}{\tau_r} \varepsilon_\phi \\
&\quad + \omega_s i_{qs} - \hat{\omega}_s \hat{i}_{qs} + \frac{F_1(e_\phi)}{L_m} \varepsilon_\phi - F_1(e_\phi) \varepsilon_d \\
&\quad + \frac{\tau_r}{L_m} \left(\frac{L_m}{\tau_r} \hat{i}_{ds} - \frac{\hat{\phi}_{dr}}{\tau_r} \right) (F_1(\hat{e}_\phi) - F_1(e_\phi)) \\
&\quad - \frac{\tau_r}{L_m} (F_1(\hat{e}_\phi) - F_1(e_\phi)) \dot{\phi}_{dr}^* + \frac{L_m}{\sigma L_s L_r \tau_r} \varepsilon_\phi
\end{aligned} \tag{48}$$

$$\begin{aligned}
d_2(\varepsilon, x, \hat{x}) &= -(k_q + a)\varepsilon_q - k_q(i_{qs}^* - \hat{i}_{qs}^*) + \hat{\omega}_s \hat{i}_{ds} - \omega_s i_{ds} \\
&\quad + \frac{PL_m}{JL_r} \hat{\phi}_{dr} \varepsilon_\Omega - \frac{L_m P}{\sigma L_s L_r} (\Omega \varepsilon_\phi + \hat{\phi}_{dr} \varepsilon_\Omega) \\
&\quad + \frac{JL_r}{L_m P \hat{\phi}_{dr}} \left(\frac{PL_m}{L_r J} \hat{i}_{qs} \hat{\phi}_{dr} - \frac{f}{J} \hat{\Omega} \right) \\
&\quad (F_2(\hat{e}_\Omega) - F_2(e_\Omega)) - \frac{PL_m}{JL_r} e_\Omega \varepsilon_\phi \\
&\quad + \frac{JL_r}{L_m P \phi_{dr} \hat{\phi}_{dr}} \left(\frac{PL_m}{L_r J} \hat{i}_{qs} \hat{\phi}_{dr} - \frac{f}{J} \hat{\Omega} \right) F_2(e_\Omega) \varepsilon_\phi \\
&\quad - \frac{JL_r}{L_m P \phi_{dr}} F_2(e_\Omega) \left(\frac{PL_m}{L_r J} i_{qs} \varepsilon_\phi - \frac{f}{J} \varepsilon_\Omega \right) \\
&\quad + F_3(\hat{e}_\Omega, \hat{\Omega}, \hat{\phi}_{dr}) - F_3(e_\Omega, \Omega, \phi_{dr}) \\
&\quad - \frac{JL_r}{L_m P \phi_{dr} \hat{\phi}_{dr}} \left(\frac{f}{J} - F_2(e_\Omega) \right) \dot{\Omega}^* \varepsilon_\phi \\
&\quad - \frac{JL_r}{L_m P \hat{\phi}_{dr}} (F_2(e_\Omega) - F_2(\hat{e}_\Omega)) \dot{\Omega}^* \\
&\quad + \frac{JL_r}{L_m P \hat{\phi}_{dr} \phi_{dr}} \hat{\Omega}^* \varepsilon_\phi - \frac{\hat{\phi}_{dr}}{\phi_{dr}} F_2(e_\Omega) \varepsilon_q
\end{aligned} \tag{49}$$

Assumption 1: The states variables of the observer (41) are bounded and remain in the operating domain \mathcal{D} for all $t \geq 0$.

From assumption 1 and 2 it can be deduced that the terms $d_1(\varepsilon, x, \hat{x})$ and $d_2(\varepsilon, x, \hat{x})$ are bounded i.e.:

$$|d_1(\varepsilon, x, \hat{x})| \leq D_1^{\max}$$

$$|d_2(\varepsilon, x, \hat{x})| \leq D_2^{\max}$$

The stability of the system (47) will be shown in two steps. First, we prove the boundedness of trajectories before the convergence of the observer (Proposition 2). Second, we prove the trajectories convergence after the convergence of the observer (Proposition 3). The boundedness of the tracking errors before the convergence of the observer, i.e. in the time domain $[0 \ t_s[$ is shown by using the development given in [35].

Proposition 2: If $k_1 \geq H_3^{\max}$, $k_2 \geq \frac{T^{\max}}{J}$, $k_3 \geq G_1^{\max} + D_1^{\max}$ and $k_4 \geq G_2^{\max} + D_2^{\max}$, then the states of the closed loop system (47) are uniformly bounded before the convergence of the observer.

Proof: To show the boundedness of the system (47) before the convergence of the observer, we use the following Lyapunov function:

$$V = \frac{1}{2}(e_d^2 + e_q^2 + e_\phi^2 + e_\Omega^2) \tag{50}$$

with $|\tanh(x)| \leq 1$ and if $k_1 \geq H_3^{\max}$, $k_2 \geq \frac{T^{\max}}{J}$, $k_3 \geq G_1^{\max} + D_1^{\max}$ and $k_4 \geq G_2^{\max} + D_2^{\max}$ we get:

$$\dot{V} \leq -k_d e_d^2 - k_q e_q^2 - k_\phi e_\phi^2 - k_\Omega e_\Omega^2 + 2k_3 |e_d| + 2k_4 |e_q| + \varepsilon_1 + \varepsilon_2 \tag{51}$$

Let $0 < \theta < 1$. Then, \dot{V} can be written as follows:

$$\begin{aligned}
\dot{V} &\leq -k_d(1 - \theta)e_d^2 - k_q(1 - \theta)e_q^2 - k_\phi(1 - \theta)e_\phi^2 \\
&\quad - k_\Omega(1 - \theta)e_\Omega^2 - k_d \theta e_d^2 + 2k_3 |e_d| - k_q \theta e_q^2 \\
&\quad + 2k_4 |e_q| - k_\phi \theta e_\phi^2 + \varepsilon_1 - k_\Omega \theta e_\Omega^2 + \varepsilon_2
\end{aligned} \tag{52}$$

Before convergence, i.e., for $t \leq t_s$, the terms e_d^2, e_q^2, e_ϕ^2 and e_Ω^2 dominate the terms $|e_d|, |e_q|, |e_\phi|$ and $|e_\Omega|$, respectively. Then, the negativity of \dot{V} can be ensured by the following conditions [35]. If: $-k_d \theta e_d^2 + 2k_3 |e_d| \leq 0$, $-k_q \theta e_q^2 + 2k_4 |e_q| \leq 0$, $-k_\phi \theta e_\phi^2 + \varepsilon_1 \leq 0$ and $-k_\Omega \theta e_\Omega^2 + \varepsilon_2 \leq 0$ i.e.: $|e_q| \geq \frac{2k_4}{k_q \theta}$, $|e_d| \geq \frac{2k_3}{k_d \theta}$, $|e_\phi| \geq \sqrt{\frac{\varepsilon_1}{k_\phi \theta}}$ and $|e_\Omega| \geq \sqrt{\frac{\varepsilon_2}{k_\Omega \theta}}$, \dot{V} becomes:

$$\begin{aligned}
\dot{V} &\leq -k_d(1 - \theta)e_d^2 - k_q(1 - \theta)e_q^2 - k_\phi(1 - \theta)e_\phi^2 \\
&\quad - k_\Omega(1 - \theta)e_\Omega^2 \quad \forall |e_q| \geq \frac{2k_4}{k_q \theta}, |e_d| \geq \frac{2k_3}{k_d \theta},
\end{aligned} \tag{53}$$

$$|e_\phi| \geq \sqrt{\frac{\varepsilon_1}{k_\phi \theta}}, |e_\Omega| \geq \sqrt{\frac{\varepsilon_2}{k_\Omega \theta}}$$

Following Definition 3, this means that the variables e_d , e_q , e_ϕ and e_Ω are uniformly bounded before the convergence of the observer. \square

The stability of the system of the tracking errors (47) after convergence of the observer, i.e., for $t \geq t_s$ is stated by the following proposition.

Proposition 3: Consider the system (47) and the observer (41), at $t = t_s$ the observer converges i.e. $\varepsilon \rightarrow 0$. Then the variables e_d , e_q , e_ϕ and e_Ω are globally uniformly exponentially practically stable.

Proof: When the observer converges ($\varepsilon = [0 \ 0 \ 0 \ 0]^T$), the perturbation terms vanish ($d_1(0, x, \hat{x}) = 0$, $d_2(0, x, \hat{x}) = 0$), for $t \geq t_s$, then the system (47) is equal to the system (33) whose stability is already proved in Proposition 1 of Section 4. \square

7. SIMULATION AND EXPERIMENTAL RESULTS

The proposed controller is tested by simulations and experimentally on a dedicated benchmark [39]. The parameters of the used IM are given in the following table:

Table 1: The IM parameters.

Nominal rate power	1.5kW
Nominal angular speed	1430 rpm
Number of pole pairs	2
Nominal voltage	220 V
Nominal current	7.5 A
R_s, R_r	1.633 Ω , 0.93 Ω
L_m, L_s, L_r	0.099H, 0.142H, 0.076H
f_v	0.0018 N.m/rad/s
J	0.0111Kg.m ²

7.1. Simulation results

In the dedicated benchmark, three reference trajectories are defined: the speed reference (Fig. 1a), load torque (Fig. 1b) and the flux reference is fixed at 0.596Wb. This benchmark permits to evaluate the performances of the proposed controller under the following operating conditions:

- Area 1.** Low speed with nominal load (from 1s to 3s).
- Area 2.** High speed with nominal load (from 4s to 6s).
- Area 3.** Very low speed with nominal load (from 7s to 9s).

The simulation was made with MATLAB/Simulink. The used sampling period is 100 μ s. The controller parameters are chosen as follows: $k_\Omega = 10$, $k_\phi = 10$, $k_1 = 100$, $k_2 = 950$, $k_3 = 100$, $k_4 = 100$, $k_d = 500$ and $k_q = 500$. The obtained simulation results are presented in Fig. 2 and Fig. 3. Fig. 2 shows the responses of the IM without parameters variations (un-faulty mode). We see that the speed and the flux trajectories converge to their desired references with good dynamics. Moreover, the load torque

is very well rejected under low and high speed. However, it appears a small static error in the speed trajectory from 7s to 9s. Also, the estimated flux and speed converge to their actual values.

To test the robustness of the proposed controller with respect to faults, we have considered the rotor resistance variation. Fig. 3 shows the responses of the IM in presence of rotor resistance variation of +100% R_r . It can be seen that the rotor resistance variation does not affect the performances of the proposed controller even in presence of the load torque.

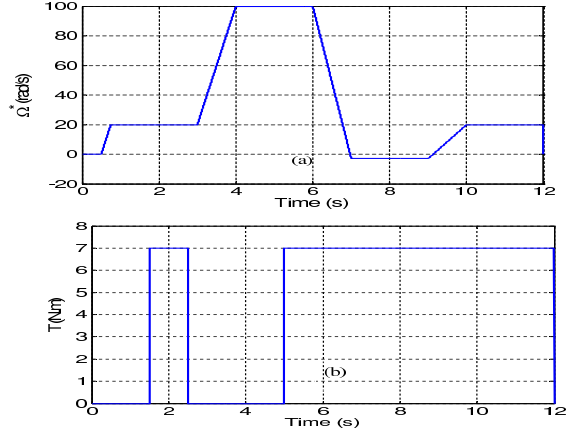


Fig 1: Benchmark trajectories

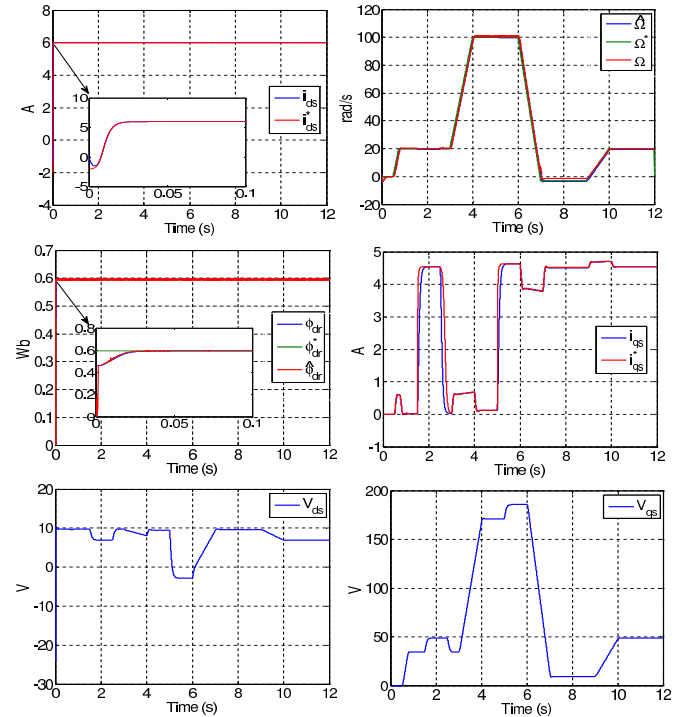


Fig 2: Simulation results without parameters variations (un-faulty mode)

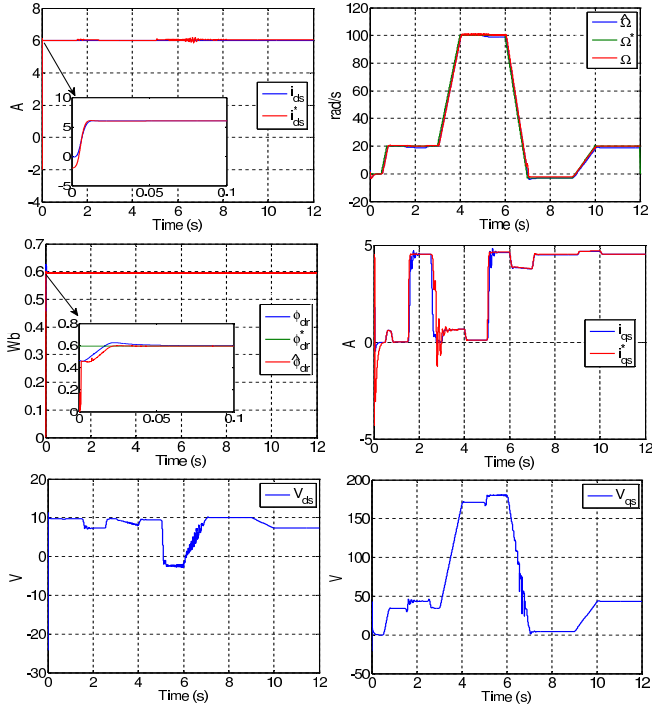


Fig 3: Simulation results with rotor resistance variations of $+100\%R_r$

7.2. Experimental results

The experimental tests have been performed at the experimental set-up (Fig. 4) located at IRCCyN at Nantes, France (see [39]). The block diagram of the proposed fault tolerant controller used in the experimental set-up is presented in Fig. 5.

The speed and the flux references considered in the experimental tests are the same as in the simulation part. However, for the load torque, practical limits have been encountered. The controller gives bad performances when the nominal load Torque (Fig. 1b) is applied. The acceptable load torque in the experimental tests is shown in Fig. 6, which exhibits chatter, due to measurement noises and electrical and electromagnetic coupling. This problem will be resolved in the future, first of all by separating the power supply of both inverters. The obtained experimental results are presented in Fig. 7 and Fig. 8. Fig. 7 shows the responses of the IM without parameters variations (the open loop identified parameters are used in the control scheme). We see that the speed and the flux trajectories track correctly their references, even if the load torque is greatly perturbed and its influence is satisfactory rejected. Nevertheless, a small static error appears when an important load torque is applied.

The robustness of the controller with respect to faults (rotor resistance variations) is tested. Fig. 8 shows the experimental results in presence of rotor resistance variations of $+100\%R_r$. Compared to the case of identified parameters, it can be seen that the controller gives the same results for

speed and flux responses, but the currents and voltages are influenced (increase in this case).

The experimental results are closed to the simulation one. Nevertheless, due to measurement noises, inverter dead time which is not taken into account, imperfection parameters knowledge (for example magnetic saturation is not considered, load torque imperfection), some differences appear.

Remark 1: Compared to the existing works already reported in the literature [30–33], the proposed sensorless robust control gives better results. Indeed, the desired performances are well achieved in presence of rotor fault for various operating conditions, i.e, for low, high and very low speed with variable load torque. Also, the proposed controller rejects the effect of the load torque despite the noisy measurement of the later (see Fig 6). At our knowledge, the combination of the backstepping control strategy with high order sliding mode observer for the design of robust sensorless controller for induction motors is not considered in the literature. Moreover, The proposed controller is validated by both simulation and experiments.



Fig 4: Experimental set-up

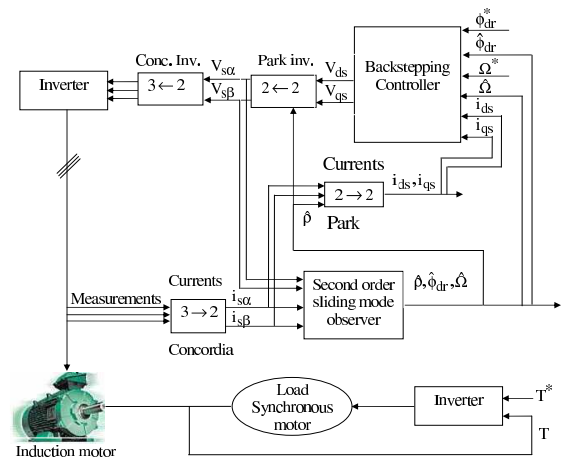


Fig 5: Block diagram of the proposed fault tolerant controller

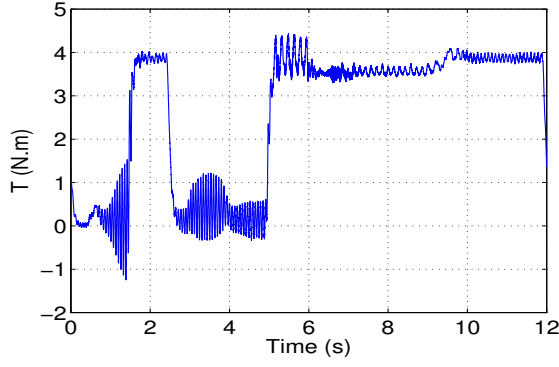


Fig 6: Measured load torque

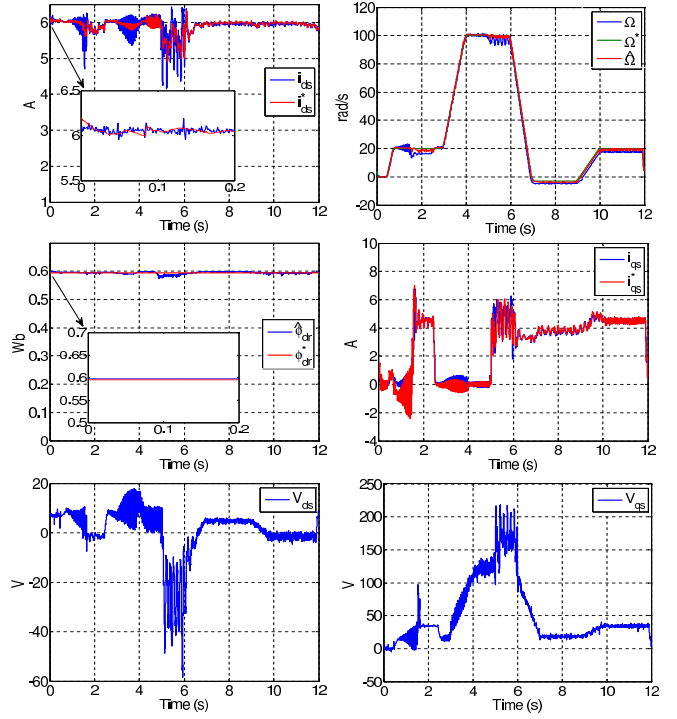


Fig 8: Experimental results with rotor resistance variations of $+100\%R_r$

8. CONCLUSION

In this paper, a sensorless fault tolerant controller for IM has been presented. First, a robust field oriented controller based on backstepping strategy is designed to steer the flux and the speed to their desired references in presence of rotor resistance variations and load torque disturbance. Second, to achieve the mechanical sensorless fault tolerant control, a second order sliding mode observer is used to estimate the speed and the flux from only the stator currents measurements. The simulation results show the robustness of the proposed control scheme. Moreover, experimental results highlight the applicability and again the robustness of the proposed control scheme even if many physical phenomena are not taken into account in our simplified control model. In our on-going work, an unbalanced case will be considered and high order (more than 2) sliding mode observer.

ACKNOWLEDGMENTS

The authors would like to thank Alain Glumineau and Robert Boisliveau for the use of the experimental set-up located at IRCCyN (see [39]). The invaluable help of Robert Boisliveau during the experimental tests of this work is gratefully acknowledged. The first author would also like to thank Mohamed Tadjine from the Laboratoire de Commandes des Processus, Ecole Nationale Polytech-

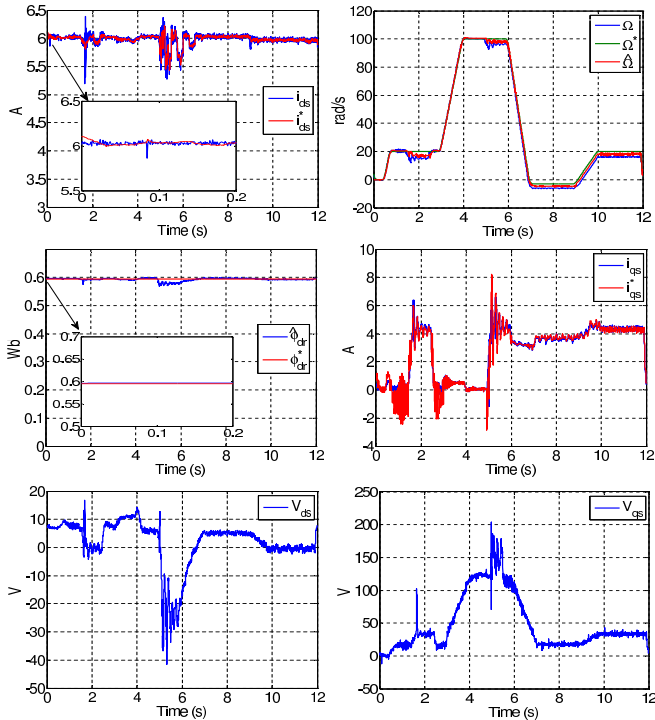


Fig 7: Experimental results without parameters variations (un-faulty mode)

nique, Algiers, Algeria, for his fruitful help.

REFERENCES

- [1] M. Blanke, M. Kinnaert, J. Lunze, and M. Staroswiecki, "Diagnostic and fault tolerant control," Springer-Verlag, 2003.
- [2] Y. Zhang, J. Jiang, "Bibliographical review on re-configurable fault-tolerant control systems," *Annual Reviews in Control*, 32, pp. 229-252, 2008.
- [3] X. G. Yan, C. Edwards, "Sensor fault detection and isolation for nonlinear systems based on a sliding mode observer," *International Journal of Adaptive Control and Signal Processing*, 21, pp. 657-673, 2007.
- [4] M.Y. Zhong, Q. Ding, P. Shi, "Parity space-based fault detection for Markovian jump systems," *International Journal of Systems Science*, 40, pp. 421-428, 2009.
- [5] A. Xu, Q. Zhang, "Nonlinear system fault diagnosis based on adaptive estimation," *Automatica*, 40, pp. 1181-1193, 2004.
- [6] Y. Zhang, H. Zhou, S. J. Qin and T. Chai, "Decentralized fault diagnosis of large-scale processes using multiblock kernel partial least squares," *IEEE Transactions on Industrial Informatics*, 6, pp. 3-10, 2010.
- [7] Y. Zhang, T. Chai, L. Zhiming and C. Yang, "Modelling and monitoring of dynamic processes," *IEEE Transactions on Neural Networks and Learning Systems*, 23, pp. 277-284, 2012.
- [8] T. Yüksel, A. Sezgin, "Two fault detection and isolation schemes for robot manipulators using soft computing techniques," *Applied Soft Computing*, 10, pp. 125-134, 2010.
- [9] D. U. Campos-Delgado, D. R. Espinoza-Trejo, E. Palacios, "Fault tolerant control in variable speed drives: a survey," *IET Electric Power Applications*, 2, pp. 121-134, 2008.
- [10] S. Bachir, S. Tnani, J. Trigeassou, and G. Champenois, "Diagnosis by parameter estimation of stator and rotor faults occurring in induction machines," *IEEE Transactions on Industrial Electronics*, 53, pp. 963-973, 2006.
- [11] I. B. A. Bazine, S. Bazine, S. Tnani, G. Champenois, "On-line broken bars detection diagnosis by parameters estimation," *13th European Conference on Power Electronics and Applications EPE*, SPAIN, Barcelona, September 8-10, 2009.
- [12] K. R. Cho, J.H. Lang, S.D. Umans, "Detection of broken rotor bars in induction motors using state and parameter estimation," *IEEE Transactions on Industry Applications*, 28, pp. 702-709, 1992.
- [13] F. Karami, J. Poshtan, M. Poshtan, "Detection of broken rotor bars in induction motors using nonlinear Kalman filters," *ISA Transactions*, 49, pp. 189-195, 2010.
- [14] S. Hedayati Kia, H. Henao, G.A. Capolino, "A high-resolution frequency estimation method for three-phase induction machine fault detection," *IEEE Transactions on Industrial Electronics*, 54, pp. 2305-2314, 2007.
- [15] T. Vaimann, A. Kallaste, "Detection of broken rotor bars in three-phase squirrel-cage induction motor using fast Fourier transform," *10th International Symposium, Topical Problems in the Field of Electrical and Power Engineering*, Pärnu, Estonia, January 10-15, pp. 52-56, 2011.
- [16] F. Filippetti, G. Franceschini, C. Tassoni, and P. Vas, "Recent developments of induction motor drives fault diagnosis using AI techniques," *IEEE Transactions on Industrial Electronics*, 47, pp. 994-1004, 2000.
- [17] N. Djeghali, M. Ghanes, S. Djennoune, J. P. Barbot, "Backstepping fault tolerant control based on second order sliding mode observer : application to induction motors," *50th IEEE Conference on Decision and Control and European Control Conference*, Orlando, Florida, Décembre 2011.
- [18] J. Holtz, "Sensorless control of induction machines with or without signal injection," *IEEE Transactions on Industrial Electronics*, 53, pp. 7-30, 2006.
- [19] C. Aurora and A. Ferrara, "A sliding mode observer for sensorless induction motor speed regulation," *International Journal of Systems Science*, 38, pp. 913-929, 2007.
- [20] M. Ghanes, and G. Zheng, "On sensorless induction motor drives: Sliding mode observer and output feedback controller," *IEEE Transactions on Industrial Electronics*, 56, pp. 3404-3413, 2009.
- [21] M. Ghanes, J. P. Barbot, J. D. Leon and A. Glumineau, "A robust sensorless output feedback controller of the induction drives: New design and experimental validation," *International Journal of Control*, 83, pp. 484-497, 2010.
- [22] C. Edwards, S. K. Spurgeon and R. J. Patton, "Sliding mode observers for fault detection and isolation," *Automatica*, 36, pp. 541-553, 2000.
- [23] T. Floquet, J. P. Barbot, W. Perruquetti and M. Djemai, "On the robust fault detection via a sliding mode disturbance observer," *International Journal of Control*, 77, pp. 622-629, 2004.
- [24] A. Levant, "Robust exact differentiation via sliding mode technique," *Automatica*, 34, pp. 379-384, 1998.
- [25] J. Davila, L. Fridman and A. Levant, "Second order sliding mode observer for mechanical systems," *IEEE Transactions on Automatic Control*, 50, pp. 1785-1789, 2005.
- [26] I. Boiko, M. I. Castellanos, L. Fridman, "Describing function analysis of second-order sliding mode observers," *International Journal of Systems Science*, 38, pp. 817-824, 2007.

- [27] T. Floquet and J. P. Barbot, "Super twisting algorithm based step by step sliding mode observers for nonlinear systems with unknown inputs," *International Journal of Systems Science*, 38, 2007.
- [28] Y. Shtessel, S. Spurgeon and L. Fridman, "Higher Order Sliding Mode Observers," *International Journal of Systems Science*, 38, pp. 771-772, 2007.
- [29] S. Solvar, V. Le, M. Ghanes, J. P. Barbot and G. Santomenna, "Sensorless second order sliding mode observer for induction motor," *IEEE International Conference on Control Applications, Part of 2010 IEEE Multi-Conference on Systems and Control*, Yokohama, Japan, pp. 1933-1938, 2010.
- [30] C. Bonivento, A. Isidori, L. Marconi and A. Paoli, "Implicit fault tolerant control: application to induction motors," *Automatica*, pp. 355-371, 2004.
- [31] D. Diallo, M. E. H. Benbouzid, A. Makouf, "A fault tolerant control architecture for induction motor drives in automotive applications," *IEEE Transactions on Vehicular Technology*, 53, pp. 1847-1855, 2004.
- [32] A. Fekih, "Effective fault tolerant control design for nonlinear systems: application to a class of motor control system," *IET Control Theory and Application*, 2, pp. 762-772, 2008.
- [33] N. Djeghali, M. Ghanes, S. Djennoune, J. P. Barbot and M. Tadjine, "Fault tolerant control for induction motors using sliding mode observers," *The 11th International Workshop On Variable Structure Systems*, Mexico City, pp. 190-196, 2010.
- [34] C. Canudas de Wit, "Commande des moteurs asynchrones 2, Optimisation, discrétisation et observateurs," Edition Hermes Science, Paris, 2000.
- [35] H. K. Khalil, *Nonlinear Systems*, 3rd Edition, Prentice-Hall, 2002.
- [36] A. Benabdallah, I. Ellouze and M. A. Hammami, "Practical stability of nonlinear time-varying cascade systems," *Journal of Dynamical and Control Systems*, 15, pp. 45-62, 2009.
- [37] C. Chen, "Backstepping control design and its applications to vehicle lateral control in automated highway systems," Ph.D. dissertation, University of California, Berkeley, 1996.
- [38] B. Yao, "Adaptive robust control of nonlinear systems with application to control of mechanical systems," Ph.D. dissertation, University of California, Berkeley, 1996.
- [39] A. Glumineau, R. Boisliveau (IRCCyN) and L. Loron (IREENA), www.irccyn.ec-nantes.fr/hebergement/BancEssai, 2008.